Temporal Coherence Behavior of a Nd:YAG Pumped Waveguide Raman Shifter

Marilou M. Cadatal*, Ma. Leilani Y. Torres, and Wilson O. Garcia
National Institute of Physics, University of the Philippines,
Diliman, Quezon City 1101
E-mail: marilou.cadatal@up.edu.ph

ABSTRACT

We study the behavior and report the control of the temporal coherence length z_c of a 355/532 nm Nd:YAG pumped H_2 Raman shifter with and without capillary waveguide (CWG). Depending on the application of the Raman-shifter light source, z_c could be tuned rapidly or slowly by varying the H_2 pressure P or the input power P_{in}. A more dynamic z_c behavior is observed for a waveguide Raman shifter.

INTRODUCTION

Stimulated Raman scattering (SRS) in H_2 is an efficient technique of extending the tuning range of lasers into the vacuum ultraviolet and far infrared (Mannik & Brown, 1986; Berry et al., 1982; Torres et al., 2003; Palero et al., 2001; Palero et al., 2000; Papayanis et al., 1998). It is simple, economical, robust, and capable of high conversion efficiency (Torres et al., 2003; Palero et al., 2001; Palero et al., 2000). Recently, the threshold energy required for SRS has been lowered and the conversion efficiency was improved by using a capillary waveguide (CWG) (Mannik & Brown, 1986; Berry et al., 1982; Torres et al., 2003).

On the other hand, laser sources with controllable temporal coherence properties are valuable in spectroscopy and optical microscopy. With its highly directional beam outputs, these sources with low coherence can be efficient illuminators in conventional optical microscopes for generating images with acceptable levels of optical noise caused by speckles, edge ringing and shifting, and point diffractions (Garcia et al., 2001). Conversely, sources with longer coherence lengths are useful in interferometric applications.

This work analyzes the temporal coherence properties of a H_2 Raman shifter with and without a CWG and demonstrates the control of its associated temporal coherence length using the H_2 pressure (P) and input power (P_{in}).

EXPERIMENTAL SETUP

The schematic diagram of the experimental setup is shown in Fig. 1. The fundamental 1064 nm output of a *Q*-switched linearly polarized neodynium-doped yttrium-aluminum-garnet (Nd:YAG) laser (Spectra Physics GCR-230) is converted to 532 nm (second harmonic) and 355 nm (third harmonic) via KDP crystals. The Nd:YAG is operating at 10 Hz repetition rate with a pulsewidth of 5–6 ns (FWHM). The telescope expands the beam before it passes through the aperture, A. Lens L_1 (f = 290 mm) focuses the beam onto the entrance of a 50-cm-long capillary tube (CWG) placed inside the Raman shifter. The capillary tube has a 1 mm bore diameter. H_2 is used as the Raman-active medium since it has the largest Raman frequency shift

*Corresponding author

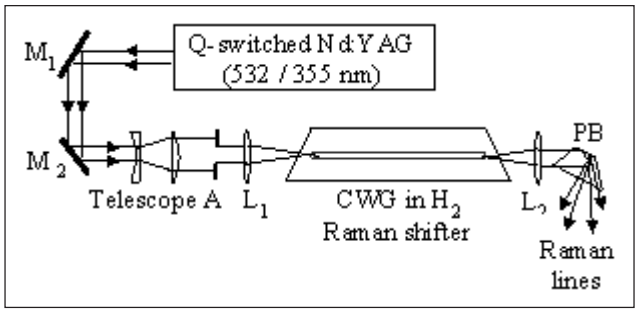

Fig. 1. Setup for the generation of Raman lines from a waveguide Raman shifter. M–mirror, L–lens, A–aperture, and PB–Pellin-Broca prism. For the conventional Raman shifter, the CWG is removed.

(4155 cm^{-1}). Lens L_2 collimates the Raman lines to the Pellin-Broca (PB) prism, which disperses the Raman output into the Rayleigh (R), Stokes (S), and anti-Stokes (AS) components. The time-averaged optical spectra $S(\lambda)$ are obtained using a grating spectrometer (SPEX Model 1000M, 3 s integration time, and 0.001 nm resolution). The power of each Raman line is measured using a power meter. This is used to normalize the spectral lines obtained from the spectrometer.

DETERMINATION OF Z_C

Since the Raman shifter is a pulsed light source, its corresponding temporal coherence length z_c is extremely difficult to measure directly with a scanning Michelson interferometer. A better technique is to employ a nonscanning multichannel Fourier transform interferometer in which the interferogram points are formed simultaneously in space, instead of through time. This requires a very fast detector array with a large number of pixels and a uniform response over a wide spectral range for a uniform sampling of the interferogram. But such a photodiode array is expensive (Garcia et al., 2001). The associated z_c of $S(\lambda)$ is determined from the following procedure proposed by Garcia et al. (2001):

Step 1: The sampled spectrum, $\{S(\lambda_m)\}$, is converted into its equivalent k representation, $\{S(k_m)\}$, where $k = 1/\lambda$; $m = 1,\ldots,M$; and k_M (cm^{-1}) = 50,000. The 355/532 nm R line is included in $\{S(\lambda_m)\}$.

Step 2: An even $(2M+1)$ data sequence, $\{S(n)\}$, is derived from $\{S(k_m)\}$, where $S(n) = S(k_m) = S(-n)$, and $n = -M,-M+1,\ldots,M$.

Step 3: The inverse Fourier transform of $S(n)$; $F^{-1}[\{S(n)\}] = I(z)$ is then obtained. Here, z is a distance variable in the range $-Mk_M \le z \le Mk_M$. $I(z)$ may be interpreted as the average interferogram generated by a Raman-shifter light source in a Michelson interferometer.

Step 4: Finally, z_c is solved with respect to $z = 0$ using:

$$z_c^2 = \int_0^\infty z^2 \Upsilon^2(z)\,dz \Big/ \int_0^\infty \Upsilon^2(z)\,dz \qquad (1)$$

Equation (1) is derived from the definition of coherence time $t_c = z_c/c$, where c is the speed of light in vacuum. Conventionally, the envelope of the interferogram $I(z)$ is first obtained and z_c is determined as the distance from $z = 0$ up to where the value of the envelope has reduced to $1/e$ (Daza et al., 1999; Born & Wolf, 1999). Using Eq. (1) permits the determination of z_c of a pulsed light source with an arbitrarily profiled emission spectrum $\{S(\lambda_m)\}$. Hence, the need to first establish the best-fit envelope of $I(z)$, which is a likely source of error, to obtain z_c is eliminated.

Z_C BEHAVIOR FOR THE 355 NM PUMP

The S and AS wavelengths generated with the 355 nm pump wavelength are summarized in Table 1.

Table 1. Generated Raman lines (λ_{pump}=355 nm).

Raman line	Wavelength (nm)	Raman line	Wavelength (nm)
S_1	415.9	AS_1	309.0
S_2	502.9	AS_2	273.8
S_3	635.9	AS_3	245.8

Samples of the $S(k)$ obtained with and without a CWG for different P at maximum P_{in} (26.5 mW) are shown in Fig. 2. Their corresponding interferograms $I(z)$ determined from Step 3 are also shown. At 150 psi with a CWG, R and S_1 lines dominate the spectrum. As the P is increased to 600 psi, S_2 and S_1 dominate and the R line is in turn depleted. Moreover, at a higher P, four-wave mixing, which is the main mechanism for AS generation, is suppressed. This leads to the depletion of the AS_1 and suppression of the AS_2 line.

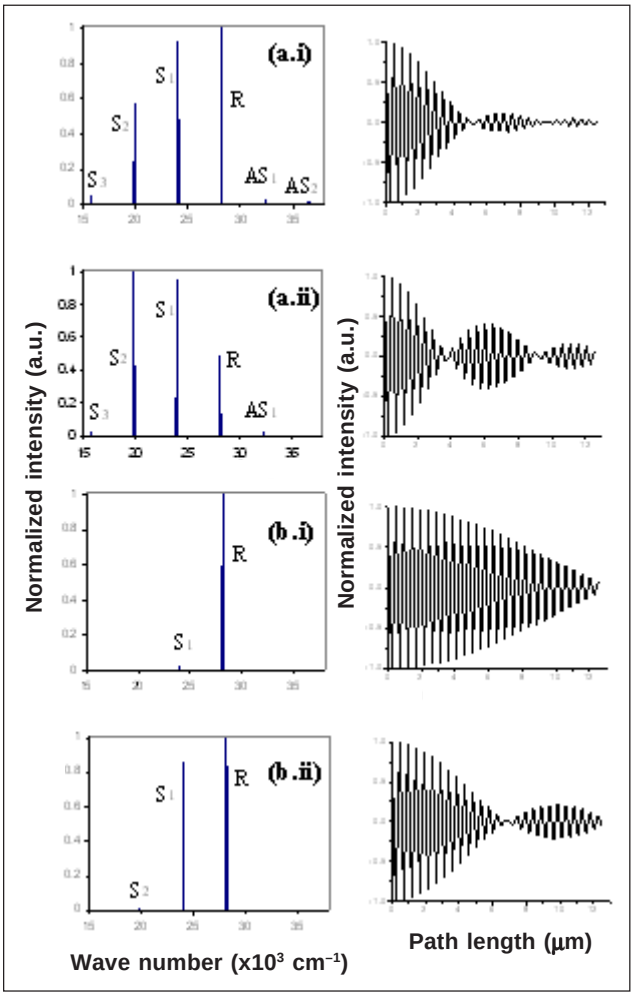

Fig. 2. On the left are the $S(k)$ for (i) P=150 psi and (ii) 600 psi (a) with and (b) without CWG. On the right are the corresponding interferograms of $S(k)$.

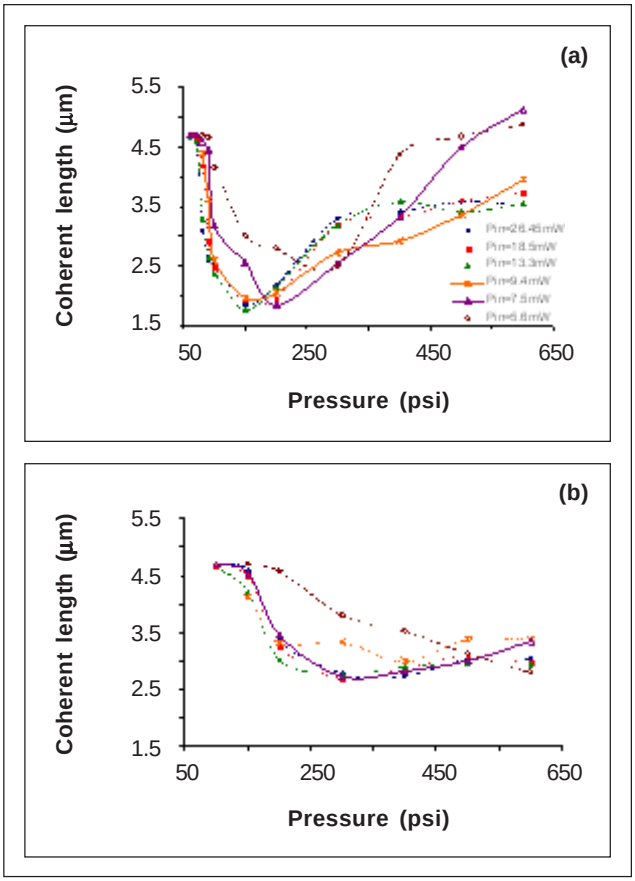

Fig. 3. z_c measurements as a function of H_2 pressure for P_{in} = 5.6, 7.5, 9.4, 13.3, 18.5, and 26.4 mW (a) with and (b) without CWG.

Hence, the bandwidth is larger and the $I(z)$ envelope is narrower at 150 psi compared with that at 600 psi. Without the CWG, only the R line dominates the spectrum at 150 psi resulting in a broad interferogram envelope. At 600 psi, although the R line still dominates, S_1 is intensified and S_2 is generated. Thus, the bandwidth of the Raman shifter is increased and the interferogram envelope narrows.

The dependence of z_c on H_2 P for different P_{in} are shown in Figs. 3(a) and 3(b) for a waveguide Raman shifter and a conventional Raman shifter, respectively. The z_c values were determined from Eq. (1).

For a waveguide Raman shifter, z_c exhibits an inverted humplike dependence on P for all P_{in}. At P_{in} = 9.4 mW, z_c could be varied from 1.97 to 4.40 mm, while at P_{in} = 26.4 mW, z_c ranges from 1.84 to 4.67 mm. For $P_{in} \geq 9.4$ mW, a stable z_c minimum is achieved at around 150 psi. At lower P_{in} (7.5 and 5.6 mW), the minimum z_c value is observed to shift to higher P.

Rapid control of z_c is possible for $P \leq 150$ psi, while a slower variation of z_c is possible for $P > 150$ psi. The z_c starts to saturate at $P \geq 300$ psi for $P_{in} > 9.4$ mW. However, z_c is not observed to saturate for $P_{in} < 9.4$ mW since at lower P_{in}, the R line dominates the spectrum.

Without the CWG [Fig. 3(b)], z_c exhibits a less pronounced inverted humplike behavior with the stable z_c minimum shifting to a higher P (300 psi) for $P_{in} \geq 9.4$ mW. For $P_{in} < 9.4$ mW, the minimum z_c value is again observed to shift to higher P. At P_{in} = 9.4 mW, z_c ranges from 2.99 to 4.68 mm, while at P_{in} = 26.4 mW, z_c could be tuned from 2.74 to 4.68 mm.

Compared with that with a CWG, a slower control of z_c is possible for P < 300 psi before reaching its minimum. For $P \geq$ 300 psi, the value of z_c starts to saturate. Moreover, a lower z_c minimum is obtained in the presence of a CWG since more lines are produced as shown in Fig. 2.

The Stokes intensity is a function of P_{in} and the H_2 P as described by (Torres et al., 2003; Palero et al., 2000)

$$I_s(l) = I_s(0)\exp(g_R I_P l) \qquad (2)$$

where I_P and $I_s(0)$ are the pump laser intensity and the initial Stokes intensity, respectively, l is the interaction length between the Raman-active medium, and g_R is the steady-state Raman gain coefficient. The g_R is proportional to the Raman-active gas P (Torres et al., 2003; Palero et al., 2000).

Without the CWG (lower l), a higher P is needed to achieve the same $I_s(l)$ at a constant I_P. However, an analysis of g_R as a function of P shows that g_R saturates as P is increased (Palero et al., 2001). Hence, even if the P is increased at a particular P_{in}, the number of Stokes lines is not increased. This leads to the saturation of the z_c value at higher P.

Figures 4(a) and 4(b) present the dependence of z_c with P_{in} with and without a CWG. In the presence of a CWG [Fig. 4(a)], the z_c value is robust against variations of $P_{in} \geq$ 10.1 mW for a particular P. For instance, at 300 psi, z_c is maintained at about 3.21 mm. For P_{in} < 10.1 mW, z_c can be controlled by varying the P_{in} at a given P or by varying the P at a given P_{in}.

Without the CWG, higher z_c values are obtained since lesser Raman lines are produced. At 100 psi, z_c is maintained at 4.69 mm since the spectrum is still dominated by the R line.

At $P \leq$ 150 psi (with CWG) and $P \leq$ 200 psi (without CWG), z_c decreases with increasing P_{in} since at low gas P, increasing P_{in} leads to the generation of more Raman lines. However, this does not work under high pressures where increasing P_{in} only results in S_2 (with CWG) and S_1 (without CWG) dominating over the Raman lines (Fig. 2).

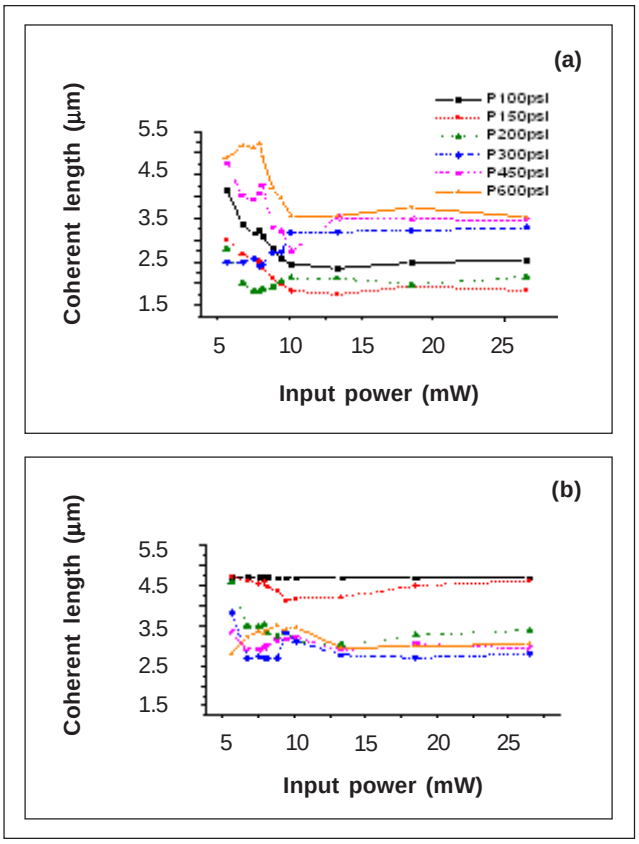

Fig. 4. z_c measurements as a function of P_{in} for H_2 pressure = 100, 150, 200, 300, 450, and 600 psi (a) with and (b) without CWG.

Z_C BEHAVIOR FOR THE 532 NM PUMP

The wavelengths of the generated Raman lines in H_2 are summarized in Table 2.

Table 2. Generated Raman lines (l_{pump} = 532 nm).

Raman line	Wavelength (nm)	Raman line	Wavelength (nm)
S_1	683.0	AS_3	319.9
AS_1	435.7	AS_4	282.3
AS_2	368.9		

Figure 5 shows the dependence of z_c on H_2 P for different P_{in} (a) with and (b) without a CWG.

As in the 355 nm pump wavelength, a rapid control of z_c is possible at certain P while a slow variation is possible for other P. A noticeable shift in the minimum z_c value

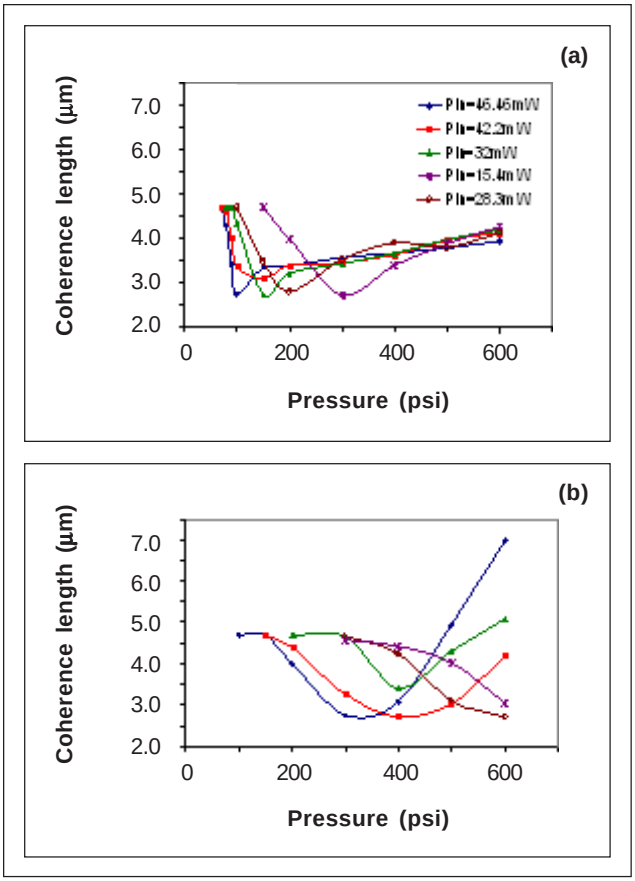

Fig. 5. z_c measurements as a function of H_2 pressure for P_{in} =15.4, 28.3, 32, 42.2, and 46.46 mW (a) with and (b) without CWG.

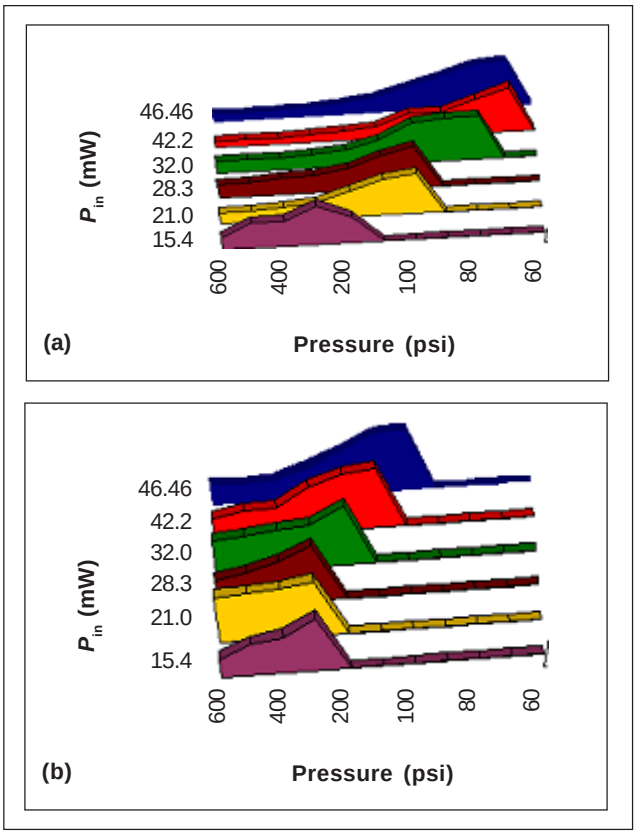

Fig. 6. Bandwidth as a function of H_2 pressure for P_{in} =15.4, 21, 28.3, 32, 42.2, and 46.46 mW (a) with and (b) without CWG.

could be observed for both waveguide and conventional Raman shifters. The shift is due to the change in the spectral bandwidth of the Raman shifter as a function of P (Fig. 6). As P_{in} decreases, more SRS lines are generated at higher P, thereby broadening the spectral bandwidth of the Raman shifter at higher P. Consequently, as P_{in} decreases, z_c minimum shifts to a higher P. While the shifting is observed for all P_{in} with a 532 nm pump wavelength, the minimum z_c is observed to shift to higher pressures only at low P_{in} for a 355 nm pump (Fig. 3). This is because the cumulative gain coefficient is inversely proportional to the pump and Stokes wavelengths (Palero et al., 2001) so that higher pump wavelengths lead to lower Stokes conversion efficiencies and higher threshold energies.

The dependence of z_c as a function of P_{in} is presented in Fig. 7. For the waveguide Raman shifter operating at 200 psi, z_c decreases for $P_{in} \leq 21$ mW due to the generation of Raman lines. However, further increase in P_{in} only results in S_1 dominating over the other Raman lines. Hence, z_c starts to increase for $P_{in} > 21$ mW. At higher P (> 200 psi), z_c increases as P_{in} is increased since an increase in P_{in} only results to S_1 dominating the spectrum. Similarly, without the CWG, z_c decreases at P_{in} where Raman lines are generated. As S_1 dominates over the spectrum, z_c increases.

CONCLUSION

The z_c of a waveguide Raman shifter can be varied over a wide range via an appropriate selection of H_2 P and P_{in}. For both 355 and 532 nm pumped waveguide Raman shifter, z_c exhibited an inverted hump behavior. For the 355 nm pumped waveguide Raman shifter, a stable z_c minimum is obtained at around 150 psi for $P_{in} \geq 9.4$ mW. If pumped with 532 nm, z_c minimum shifts to higher pressures for decreasing P_{in}. Lower z_c values could be obtained by a waveguide Raman shifter.

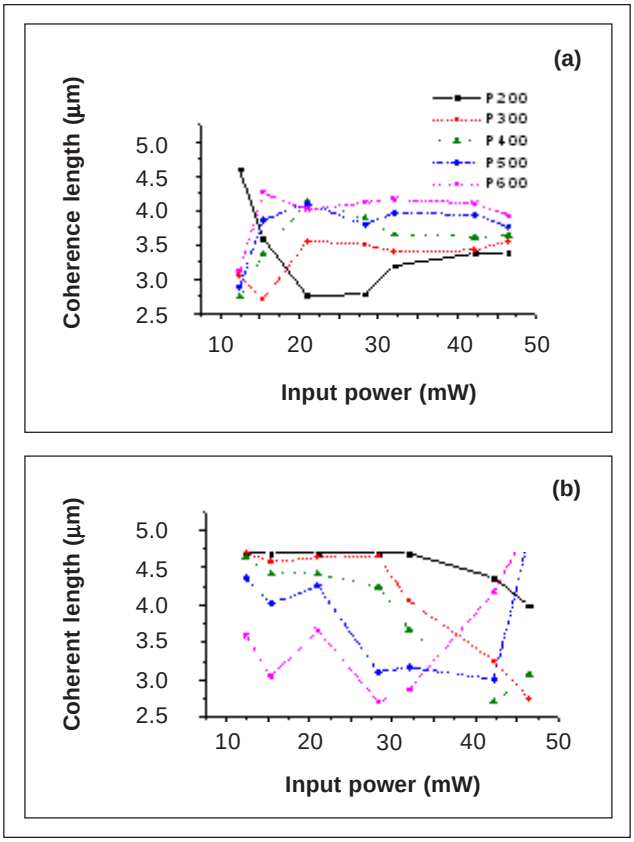

Fig. 7. z_c measurements as a function of P_{in} for H_2 pressure =200, 300, 400, 500, and 600 psi (a) with and (b) without CWG.

ACKNOWLEDGMENTS

The authors gratefully acknowledge the Instrumentation Physics Laboratory of the National Institute of Physics for lending the detector used in this work and the Philippine Department of Science and Technology (DOST) through the Engineering and Science Education Project (ESEP) for the equipment grant. This project is supported by the University of the Philippines and the Philippine Council for Advanced Science and Technology Research and Development (PCASTRD).

REFERENCES

Berry, A.J., D.C. Hanna, & D.B. Hearn, 1982. Low threshold operation of a waveguide H_2 Raman laser. *Opt. Commun.* **43**: 229–232.

Born, M. & E. Wolf, 1999. Principles of optics, 7th ed. Cambridge University Press, Cambridge.

Daza, M.R., A. Tarun, K. Fujita, & C. Saloma, 1999. Temporal coherence behavior of a semiconductor laser under strong optical feedback. *Opt. Commun.* **161**: 123–131.

Garcia, W., J. Palero, & C. Saloma, 2001. Temporal coherence control of Nd:YAG pumped Raman shifter. *Opt. Commun.* **197**: 109–114.

Mannik, L. & S.K. Brown, 1986. Tunable infrared generation using third Stokes output from a waveguide Raman shifter. *Opt. Commun.* **57**: 360–364.

Palero, J.A., J.O.S. Amistoso, M.F. Baclayon, & W.O. Garcia, 2000. Generation of UV, VIS, and NIR laser light by stimulated Raman scattering in hydrogen with a pulsed 355 nm Nd:YAG laser. *Proceedings of the 18th SPP Philippine Physics Congress.*

Palero, J.A., R.S. Ibarreta, & W.O. Garcia, 2001. Frequency conversion of a 532 nm Nd:YAG laser using a hydrogen Raman shifter. *Proceedings of the 19th SPP Philippine Physics Congress.*

Papayanis, A.D., G.N. Trikrikas, & A.A. Serafetinides, 1998. Generation of UV and VIS laser light by stimulated Raman scattering in H_2, D_2, and H_2/He using a pulsed Nd:YAG laser at 355 nm. *Appl. Phys. B.* **67**: 563–568.

Torres, M.L., M. Cadatal, & W. Garcia, 2003. Stimulated Raman scattering in a 532 nm Nd:YAG laser pump hydrogen Raman shifter with a capillary waveguide. *Proceedings of the 21st SPP Philippine Physics Congress.*